HHS Public Access

Author manuscript

Mol Cell Neurosci. Author manuscript; available in PMC 2017 March 01.

Published in final edited form as:

Mol Cell Neurosci. 2016 March ; 71: 1–12. doi:10.1016/j.mcn.2015.12.003.

Novel Axon Projection after Stress and Degeneration in the *Dscam* Mutant Retina

K.A. Fernandes[1], **S. J. Bloomsburg**[2], **C. J. Miller**[2], **S. A. Billingslea**[2], **M. M. Merrill**[2], **R. W. Burgess**[3], **R.T. Libby**[1], and **P. G. Fuerst**[2,4]

[1] Flaum Eye Institute, University of Rochester Medical Center, Rochester, NY 14642, USA.

[2] University of Idaho Department of Biological Sciences, Moscow, Idaho, 83844, USA.

[3] The Jackson Laboratory, Bar Harbor, ME 04609, USA.

[4] WWAMI Medical Education Program, Moscow, Idaho, 83844, USA.

Abstract

The Down syndrome cell adhesion molecule gene (*Dscam*) is required for normal dendrite patterning and promotes developmental cell death in the mouse retina. Loss-of-function studies indicate that *Dscam* is required for refinement of retinal ganglion cell (RGC) axons in the lateral geniculate nucleus, and in this study we report and describe a requirement for *Dscam* in the maintenance of RGC axon projections within the retina. Mouse *Dscam* loss of function phenotypes related to retinal ganglion cell axon outgrowth and targeting have not been previously reported, despite the abundance of axon phenotypes reported in *Drosophila* Dscam1 loss and gain of function models. Analysis of the *Dscam* deficient retina was performed by immunohistochemistry and western blot analysis during postnatal development of the retina. Conditional targeting of *Dscam* and *Jun* was performed to identify factors underlying axon-remodeling phenotypes. A subset of RGC axons were observed to project and branch extensively within the *Dscam* mutant retina after eye opening. Axon remodeling was preceded by histological signs of RGC stress. These included neurofilament accumulation, axon swelling, axon blebbing and activation of JUN, JNK and AKT. Novel and extensive projection of RGC axons within the retina was observed after upregulation of these markers, and novel axon projections were maintained to at least one year of age. Further analysis of retinas in which *Dscam* was conditionally targeted with *Brn3b* or *Pax6α* Cre indicated that axon stress and remodeling could occur in the absence of hydrocephalus, which frequently occurs in *Dscam* mutant mice. Analysis of mice mutant for the cell death gene *Bax*, which executes much of *Dscam* dependent cell death, identified a similar axon misprojection phenotype. Deleting *Jun* and *Dscam* resulted in increased axon remodeling compared to *Dscam* or *Bax* mutants. Retinal ganglion cells have a very limited capacity to regenerate after damage in the adult retina, compared to the extensive projections made

Correspondences to: Peter G. Fuerst, 145 Life Science South, Department of Biological Sciences, University of Idaho, Moscow, Idaho 83844. fuerst@uidaho.edu.

in the embryo. In this study we find that DSCAM and JUN limit ectopic growth of RGC axons, thereby identifying these proteins as targets for promoting axon regeneration and reconnection.

Keywords

Cell death; regeneration; optic nerve; axon crush; plasticity

Introduction

Damage to retinal ganglion cells (RGCs) and their axons results in visual impairment and blindness, but only limited progress has been made in cell therapy approaches to replace lost RGCs or in stimulating regrowth of RGC axons. Analysis of signaling events in glaucoma mouse models and optic nerve crush, a commonly used acute model for glaucoma (Allcutt et al., 1984a, b), has identified changes in the activation status of JUN, JNK, DLK and AKT as mediators of subsequent cell death and as potential mediators of axon regrowth (Duan et al., 2015; Koistinaho et al., 1993; Watkins et al., 2013). An outstanding question is the nature of the pathways that are activated by these stresses. For example JUN and JNK signaling is involved in cell stress, remodeling and regeneration, and cell death (Fernandes et al., 2012; Vander and Levkovitch-Verbin, 2012; Yoshida et al., 2002), suggesting that upregulation of these pathways may serve to activate an axon remodeling and regenerative response, followed by cell death if this process fails.

In this study we examine RGC stress pathways and maintenance of the RGC axon in the *Dscam* mutant retina. The Down syndrome cell adhesion molecule (DSCAM) protein is a homophilic cell adhesion molecule (Agarwala et al., 2000; Yamakawa et al., 1998) that also serves as a receptor for the axon guidance molecule netrin (Liu et al., 2009; Ly et al., 2008). The *Dscam* gene is required for several features of normal retinal development including: developmental cell death (Fuerst et al., 2008), lamination (Yamagata and Sanes, 2008), dendrite-refinement (Li et al., 2015), and to prevent clustering of cell bodies and dendrites (Fuerst et al., 2009). Axons of *Dscam* mutant RGCs project normally to the optic nerve head (Fuerst et al., 2009), suggesting that alternative netrin receptors guide RGC axons out of the retina (Deiner et al., 1997). Defects in refinement and segregation of RGC axon terminals in the *Dscam* mutant brain have been described, indicating that *Dscam* plays a role in both axon and dendrite organization in retinal neurons (Blank et al., 2011).

Here we report that activation of the stress pathway proteins JUN, JNK and AKT occurs in the postnatal *Dscam* mutant retina, but with a different outcome following stress and axon degeneration compared to other RGC stress and damage models: remodeling and projection of new RGC axons. Axons target the optic disc but fail to exit, and project extensively through the *Dscam* mutant retina.

Methods

Animal Care and Handling

Mice were housed on a 12-hour light dark cycle and fed *ad libitum*. Mice taken for study were anesthetized with tribromoethanol and perfused with phosphate buffered saline, pH

7.4. Retinas were hemisected and fixed in 4% buffered PFA at room temperature for 2-4 hours. All procedures were performed in accordance with the respective University of Idaho, Jackson Laboratory or Rochester Animal Care and Use Committees.

Mutant and Transgenic Mouse Lines and Genotyping

Dscam^{del17}, *Dscam*^{2J}, *Dscam*^{F} and *Dscam*^{FD} mice (truncation, protein null, conditional and germ line-targeted conditional, respectively) were genotyped as previously described (Fuerst et al., 2012; Fuerst et al., 2010; Fuerst et al., 2008). *Dscam*^{del17}, *Dscam*^{2J} and *Dscam*^{FD} mice are collectively referred to as *Dscam*^{LOF} (loss of function) unless otherwise noted. YFPH mice were acquired from The Jackson Laboratory's and genotyped according to JAX protocols. *Pax6α*-Cre mice (generous gift of Dr. Gruss) and *Brn3b*-Cre mice (generous gift of Dr. Van Bennet) were genotyped by PCR for the presence of the Cre gene. The floxed allele of *Jun* was a generous gift of Dr. Behrens (Behrens et al., 2002). Ai9 and tdtomato/GFP reporter mice were acquired from The Jackson Laboratory and genotyped according to JAX protocols.

Retina Sectioning

Fixed retinas were sucrose sunk in 30% buffered sucrose for 1 hour, followed by an additional 30 minutes in 50% buffered sucrose and 50% optimal cutting temperature (OCT) reagent (Tekura Inc). Retinas were frozen in 100% OCT reagent and cut at 10 μm on a cryostat.

Controlled optic nerve crush (CONC): Optic nerve injury was performed as previously described (Harder and Libby, 2011; Libby et al., 2005). In brief, optic nerves were crushed for approximately 5 seconds just behind the eye using self-closing forceps (Roboz RS-5027). Eyes were harvested at 1 day following CONC to assess JUN upregulation.

Immunohistochemistry

Tissues were incubated in a blocking solution consisting of 7.5% normal donkey serum, 0.1% triton x-100 (sections) or 0.4% triton x-100 (whole retinas) and 0.02% sodium azide, diluted in phosphate buffered pH 7.4 saline (PBS). Antibodies were diluted in blocking solution. Sections were incubated with primary antibody for two hours (at room temperature) or overnight (at 4 °C). Sections were washed 2x for 15 minutes in PBS. Secondary antibodies, which were diluted in blocking solution, were applied for two hours at room temperature, followed by three ten minute washes in PBS. The second wash was supplemented with DAPI reagent to stain nuclei at a dilution of 1:50,000 of a 1 mg/ml stock. Whole retinas were stained in a similar fashion except they were blocked for one hour and antibodies were incubated for four days (primary) and three days (secondary), and washes were carried out for two hours at 4°C. Tissues were mounted on slides with 80% glycerol, in 1x PBS, containing 0.02% sodium azide, and imaged on an Olympus IX81 inverted microscope.

Western Blot Analysis

Retinas were homogenized in t-per buffer (Thermo Scientific) supplemented with protease inhibitors and EDTA (Thermo Scientific). Protein concentrations were determined using

Bradford analysis. Polyacrylamide gel electrophoresis and western blotting were performed as described previously (Schramm et al., 2012). Band densities were compared using image J software.

Dextran and cholera toxin injection

Cy3-conjugated dextran (10,000 kDA; Life Technologies) was injected into the superior colliculus of mice at postnatal day 8 (P8). Retinas were collected for study at P16. 2 μl of cholera toxin conjugated to alexa-568 (Life Technologies) was injected into a single eye of mice between the ages of P28 and six months. Mice were taken for study two days later.

Nearest Neighbor analysis

Nearest neighbor analysis was performed as previously described using the program winDRP (de Andrade et al., 2014; Keeley and Reese, 2014; Rockhill et al., 2000; Wassle and Riemann, 1978). Soma size was set at 10 μm, with 25 10 μm bins selected for analysis.

Antibodies Used

The following antibodies were used in this study for immunohistochemistry: JUN (Abcam, catalog number ab40766: 1:250), β-III tubulin (the antigen recognized by the TUJ1 antibody) (Sigma Aldrich, catalog number: SDL3D10: 1:1,000), Neurofilament (Developmental Studies Hybridoma Bank, catalog number 2H3: 1:50), AP2α (Developmental Studies Hybridoma Bank, catalog number 3B5 concentrate: 1:50). Fluorescent secondary antibodies directed to the appropriate species were used (Jackson Immuno Research, 1:500).

The following antibodies were used for western blotting: pJUN (Cell Signaling Technology, catalog number D47G9: 1:1,000), JUN (Cell Signaling Technology, catalog number 9165: 1:1,000), JNKP (Cell Signaling Technology, catalog number 9251: 1:500), AKT473 (Cell Signaling Technology, catalog number 4060: 1:1,000), AKT (Cell Signaling Technology, catalog number 4691: 1:1000), GADPH (Synaptic Systems, catalog number 247 002: 1:1,000) and goat anti-rabbit:HRP (Cell Signaling Technology, catalog number 7074: 1:25,000).

Results

Postnatal Axon Remodeling Phenotypes in *Dscam* mutant mice

The axons of RGCs project across the surface of the retina to the optic disc, where they exit the eye and target loci in the rest of the brain. RGC axons projected out of the $Dscam^{LOF}$ retina normally during development (Fuerst et al., 2009); however, RGC axons projecting aberrantly within the adult $Dscam^{LOF}$ retina were subsequently observed (Figure 1 A and B). These axons branch multiple times within the retina (Figure 1 C) and course through the synaptic layers of the retina (Figure 1 D). The developmental timing of this phenotype was assayed. Misdirected RGC axons were not observed before eye opening (Figure 1 E). Shortly after eye opening (P14), at postnatal day 16 (P16), the first indication of RGC axon abnormality within the retina was observed: swollen and blebbing (degenerating) axons (Figure 1 F), accumulation of neurofilament-m (NF) in the soma of RGCs (Figure 1 F),

RGCs with contorted or branched axons (Figure 1 G) or severed axons (Figure 1 H), and axons that terminated in a degenerated end bulb disconnected from the RGC soma (Figure 1 I). Significant increases in the number of swollen axons (Figure 1 F arrowhead), axon torpedoes (Figure 1 G arrows), NF swollen soma (Figure 1 F asterisks) and disconnected axons (Figure 1 I arrowheads) were detected comparing wild type and *Dscam*^{LOF} retinas at postnatal day 16 (Figure 1 J). These phenotypes were observed in all assayed *Dscam* mutant strains, including *Dscam*^{del17}, *Dscam*^{2J} and *Dscam*^{FD} mutant mice (data not shown). These results indicate that RGC axons undergo a process of degeneration and remodeling in the *Dscam*^{LOF} retina coincident with the time that visual circuitry just starts receiving light input at approximately P14.

Axon swelling in the adult retina originated at the optic disc, with swollen axons then projecting and branched in the peripheral retina (Figure 2 A-D; quantified in Table 1). A small number of RGC axons sample the contralateral optic nerve in the developing chick retina (McLoon and Lund, 1982) and RGC axons have been observed projecting across the optic chiasm and towards the opposite eye in a model of axon regeneration (Sun et al., 2011). Fluorescently labeled cholera toxin was injected into a single eye to test if axons were projecting into the opposite retina from the injected eye. The optic nerve and retina of the injected eye were filled with dye (Figure 2 E-G). No dye was observed in the contralateral optic nerve or retina (Figure 2 H and I), despite the dye reaching distal targets such as the lateral geniculate nucleus and superior colliculus (Figure 2 H and data not shown). This indicated that axons from one eye do not innervate the contralateral eye in *Dscam*^{LOF} mice.

To better understand the nature of RGC axon remodeling phenotypes in *Dscam*^{LOF} mice, we labeled RGCs using the YFPH transgene, which expresses YFP very brightly in a small number of RGCs (Feng et al., 2000). Labeling of individual axons revealed that a single RGC could project an axon throughout most of the retina (Figure 3 A). Two misprojecting axons labeled with the YFPH were identified in over 20 mutant retinas carrying the YFPH transgene. These axons targeted the optic disc, but then turned around and projected within the retina (Figure 3 B). After initially turning around at the optic disc, abnormal axons branched extensively within the retina and failed to retarget the optic disc (Figure 3 C). To test if RGCs showing evidence of axon damage (somal neurofilament accumulation, axon blebbing or no discernable axon) projected axons that reached the brain during development, we injected fluorescently labeled dextran into the superior colliculus of *Dscam*^{LOF} mice at postnatal day 8 (P8), which was transported to the cell soma in the retina. By P16, cells that accumulated neurofilament had dextran in their cell soma, indicating that their axons had reached this target (Figure 3 D-G). These results indicate that the RGCs that demonstrate signs of axonal stress in adult *Dscam*^{LOF} retinas were not cells that had failed to innervate central targets.

Hydrocephalus does not cause RGC Stress in *Dscam* deficient RGCs

Dscam^{LOF} mice often have severe hydrocephalus (Xu et al., 2011) that damages the central targets of RGCs, and could underlie RGC stress and axon remodeling. To determine if RGC stress and axon remodeling observed in *Dscam*^{LOF} mice occur as a result of hydrocephalus,

Dscam was conditionally deleted in RGCs using *Brn3b*-Cre, which is expressed in the midbrain and retina (Figure 4 A). No hydrocephalus was observed in *Brn3b-cre*; $Dscam^{fl/fl}$ mice (data not shown). Axon remodeling was still observed when *Dscam* was deleted with *Brn3b*-Cre compared to controls (Figure 4 B and C; quantified in Table 1) indicating that these responses are not dependent on hydrocephalus. Similar results were observed when *Dscam* was targeted with *Pax6α*-Cre, in which there is little recombination in the brain (data not shown) (Stacy and Wong, 2003).

Axon misprojection is observed in *Bax* deficient retinas

Bax deficient mice share many phenotypes in common with $Dscam^{LOF}$ *mice*, including dendrite clumping and a reduction in RGC developmental cell death (Chen et al., 2013; Keeley et al., 2012; Li et al., 2015) (Figure 5 A). Therefore we tested if the *Bax* null retina phenocopied RGC axon remodeling phenotypes observed in the *Dscam* mutant retina. Axon misprojection phenotypes were also observed in the *Bax* mutant retina (Figure 5 B; quantified in Table 1). These results suggest that the axon remodeling observed in the $Dscam^{LOF}$ and $Bax^{-/-}$ retinas could be a secondary effect from a failure of RGCs to undergo developmental cell death.

Activation of Stress Response Proteins

RGC axon stress results in the concomitant activation of cell survival (AKT) (Koriyama et al., 2006; Nakazawa et al., 2003) and cell death (JNK) signaling pathways (Fernandes et al., 2012; Yang et al., 2015). To test if these pathways were activated in $Dscam^{LOF}$ mice we assayed the phosphorylation status of JUN, JNK and AKT by western blot analysis before, during, and after onset of RGC stress. Increased phosphorylation of JUN, JNK and AKT was observed in the $Dscam^{LOF}$ retina compared to wild type (Figure 6). Quantification of these results confirmed that JUN (quantified at P14), JNK (quantified at P18) and AKT (quantified at P18) phosphorylation levels were significantly increased in the $Dscam^{LOF}$ retina compared to wild type ($P<0.006$, $P=0.02$ and $P<0.01$, respectively).

To determine if the JNK signaling pathway is activated cell intrinsically in RGCs, co-labeling of JUN was preformed along with an RGC marker, TUJ1 (Cui et al., 2003; Robinson and Madison, 2004). Following its phosphorylation by JNK, JUN is known to get activated and upregulate the expression of several genes, one of which is JUN itself (Angel et al., 1988; Pulverer et al., 1991). Since commercially available pJUN antibodies are not specific for pJUN by immunohistochemistry (Fernandes et al., 2012), the accumulation status of JUN was assessed as a surrogate of JUN activation. JUN appeared to be upregulated in a subset of RGCs labeled with TUJ1 in the $Dscam^{LOF}$ retinal ganglion cell layer (Figure 7 A and B). Interestingly, consistent with some but not all RGCs showing signs of axonal stress, not all TUJ1-positive RGCs were JUN-positive in $Dscam^{LOF}$ retinas. Additionally, the level of JUN upregulation observed in $Dscam^{LOF}$ retinas appeared to be lower than that observed in RGCs after an acute axonal injury, controlled optic nerve crush (Figure 7 C).

To determine the developmental timing of JUN upregulation, $Dscam^{LOF}$ and control retinas were immunolabeled for JUN at and after the onset of axon stress remodeling. Cells positive

for JUN were observed as early as P9 in *Dscam*^{LOF} retinas (Figure 8 A and B), and the intensity of JUN labeling appeared to increase in RGCs at P13 and P18 (Figure 8 C-F), with occasional JUN positive RGCs observed in the adult retina (Figure 8 G and H). Quantification of values indicated a significant increase in the number of JUN+ cells in the *Dscam*^{LOF} retina compared to wild type after P9, and a significant increase in JUN+ cells when comparing *Dscam*^{LOF} retinas at P13 to *Dscam*^{LOF} retinas at other ages (Figure 8 I). A significant increase in displaced cells was also detected and found to increase in the mutant genotype after P9 (Figure 8 J).

JUN knockout exacerbates axon remodeling phenotypes observed in *Dscam* deficient retinas

JUN is known to function in several processes including axon regeneration, cell survival and death and is required for efficient regeneration of peripheral axons (Fernandes et al., 2012; Hettinger et al., 2007; Raivich et al., 2004; Watkins et al., 2013). Since JUN was activated during the time window when axon remodeling is observed in the *Dscam* null retinas, *Dscam*/*Jun* double knockout retinas (DKO) were generated to test if JNK-JUN-mediated stress promoted axon remodeling, or if this was simply a correlation. Quantification revealed that increased axon remodeling was observed in the DKO retina, indicating that JUN is not required for the axon remodeling observed in *Dscam*^{LOF} mice and that its elimination results in an increased number of remodeled axons (Figure 9 A-F).

A prominent phenotype observed in the *Dscam*^{LOF} retina is the cell type specific clumping of dendrites of TH-positive dopaminergic amacrine cells (DACs) in the IPL. Dendrite clumping phenotypes associated with *Dscam* loss-of-function were observed in the *Dscam*/*Jun* DKO retinas (Figure 9 G-I). Nearest neighbor analysis was performed to quantify spacing of DACs. Nearest neighbor analysis is a measurement of the distance to the nearest cell of the same type, and measures the tendency of cells to space themselves with respect to cells of the same type. Significant differences were detected comparing wild type DACs to either *Dscam*^{LOF} or DKO retinas, but significant differences were not detected when comparing *Dscam*^{LOF} to DKO retinas (Figure 9 K-P).

Lamination of dendrites in wild type retinas and *Dscam*^{LOF} or *Dscam*/*Jun* mutant retinas was imaged. Laminar disorganization observed in the *Dscam*^{LOF} retina was also observed in the *Dscam*/*Jun* double mutant retina (Figure 10 A-I).

Discussion

In this study we report a requirement for *Dscam* in RGC axon organization within the retina. We find that markers of cell stress are upregulated in RGCs of the *Dscam*^{LOF} retina shortly before eye opening, followed by axon degeneration and remodeling. Axon remodeling involved projection of RGC axons throughout the retina. Dscams have previously been implicated in promoting the organization of retinal dendrites and this study identifies a novel role in RGC axon homeostasis.

DSCAM proteins are perhaps best known for their role in providing dendrite self-avoidance cues. This is exemplified by *Drosophila* Dscam1, which is alternatively spliced into tens of

thousands of potential isoforms (Schmucker et al., 2000), each capable of mediating homotypic binding (Chen et al., 2006; Neves and Chess, 2004). Differential expression of these isoforms permits cell specific identification and avoidance of a given cell's dendrites (Hattori et al., 2007; Hughes et al., 2007). Dscams in the mouse retina have previously been reported to guide dendrite lamination (Li et al., 2015) and are required to prevent ectopic clumping of cell bodies and dendrites in the mouse retina (Fuerst et al., 2009). The prevention of cell and dendrite clumping in the mouse retina occurs within cell types, consistent with the lack of extensive alternative splicing of vertebrate Dscams (Agarwala et al., 2000; Yamakawa et al., 1998). In addition to promoting dendrite organization, roles for Dscam1 in axon development have been described in *Drosophila*, where *Dscam* is required for axon targeting (Hummel et al., 2003; Schmucker et al., 2000; Wang et al., 2002) and regulation of axon branching (He et al., 2014). DSCAM also binds the axon guidance molecule netrin and has been shown to play a role in axon path finding in a number of vertebrate species: including chick (Ly et al., 2008), mouse (Liu et al., 2009), zebrafish (Yimlamai et al., 2005) and *Xenopus* (Morales Diaz, 2014). *Dscam* dosage has been shown to regulate synaptic organization (Cvetkovska et al., 2013; Kim et al., 2013), but requirements in axon maintenance have not previously been reported.

Analysis of *Bax* mutant retinas, which phenocopy dendrite organization (Chen et al., 2013; Keeley et al., 2012) and cell death defects (Deckwerth et al., 1996) and the axon remodeling phenotype reported here, suggest that DSCAM-dependent interactions within the retina result in the removal of cells, which then remodel axons in the absence of *Dscam* or *Bax*. Our data indicate that JUN signaling is not required for axon remodeling in *Dscam* mutant mice, but rather an increase in the number of misprojected axons was observed in the *Dscam*/*Jun* double mutant, suggesting that JUN signaling inhibits this type of axonal plasticity. Activation of AKT, which promotes axon RGC regeneration (Duan et al., 2015), was also observed, consistent with the novel axonal projections observed within the *Dscam* mutant retina.

Conclusion

The axons of retinal ganglion cells undergo a process of degeneration and regrowth after the onset of visual function in *Dscam* mutant mice. Remodeling is retina-autonomous, initiated by RGC-intrinsic events and is phenocopied in the *Bax* mutant retina. The timing of axon stress and remodeling is coincident with activation of JUN and AKT. JUN-dependent signaling is not required for the axon remodeling and in its absence a significant increase in the number of novel axon projections was observed.

Acknowledgements

This research was supported by the National Eye Institute Grant EY020857 (Fuerst), EY018606 (Libby) and an unrestricted grant to the Rochester Department of Ophthalmology from Research to Prevent Blindness. Imaging support was provided by NIH Grant Nos. P20 RR016454, P30 GM103324-01 and P20 GM103408. Duy Nguyen, Dee Schramm and Aaron Simmons assisted with experiments.

References

Agarwala KL, Nakamura S, Tsutsumi Y, Yamakawa K. Down syndrome cell adhesion molecule DSCAM mediates homophilic intercellular adhesion. Brain Res Mol Brain Res. 2000; 79:118–126. [PubMed: 10925149]

Allcutt D, Berry M, Sievers J. A qualitative comparison of the reactions of retinal ganglion cell axons to optic nerve crush in neonatal and adult mice. Brain Res. 1984a; 318:231–240. [PubMed: 6498499]

Allcutt D, Berry M, Sievers J. A quantitative comparison of the reactions of retinal ganglion cells to optic nerve crush in neonatal and adult mice. Brain Res. 1984b; 318:219–230. [PubMed: 6498498]

Angel P, Hattori K, Smeal T, Karin M. The jun proto-oncogene is positively autoregulated by its product, Jun/AP-1. Cell. 1988; 55:875–885. [PubMed: 3142689]

Behrens A, Sibilia M, David JP, Mohle-Steinlein U, Tronche F, Schutz G, Wagner EF. Impaired postnatal hepatocyte proliferation and liver regeneration in mice lacking c-jun in the liver. EMBO J. 2002; 21:1782–1790. [PubMed: 11927562]

Blank M, Fuerst PG, Stevens B, Nouri N, Kirkby L, Warrier D, Barres BA, Feller MB, Huberman AD, Burgess RW, Garner CC. The Down syndrome critical region regulates retinogeniculate refinement. J Neurosci. 2011; 31:5764–5776. [PubMed: 21490218]

Chen BE, Kondo M, Garnier A, Watson FL, Puettmann-Holgado R, Lamar DR, Schmucker D. The molecular diversity of Dscam is functionally required for neuronal wiring specificity in Drosophila. Cell. 2006; 125:607–620. [PubMed: 16678102]

Chen SK, Chew KS, McNeill DS, Keeley PW, Ecker JL, Mao BQ, Pahlberg J, Kim B, Lee SC, Fox MA, Guido W, Wong KY, Sampath AP, Reese BE, Kuruvilla R, Hattar S. Apoptosis regulates ipRGC spacing necessary for rods and cones to drive circadian photoentrainment. Neuron. 2013; 77:503–515. [PubMed: 23395376]

Cui Q, Yip HK, Zhao RC, So KF, Harvey AR. Intraocular elevation of cyclic AMP potentiates ciliary neurotrophic factor-induced regeneration of adult rat retinal ganglion cell axons. Mol Cell Neurosci. 2003; 22:49–61. [PubMed: 12595238]

Cvetkovska V, Hibbert AD, Emran F, Chen BE. Overexpression of Down syndrome cell adhesion molecule impairs precise synaptic targeting. Nat Neurosci. 2013; 16:677–682. [PubMed: 23666178]

de Andrade GB, Long SS, Fleming H, Li W, Fuerst PG. DSCAM localization and function at the mouse cone synapse. J Comp Neurol. 2014; 522:2609–2633. [PubMed: 24477985]

Deckwerth TL, Elliott JL, Knudson CM, Johnson EM Jr. Snider WD, Korsmeyer SJ. BAX is required for neuronal death after trophic factor deprivation and during development. Neuron. 1996; 17:401–411. [PubMed: 8816704]

Deiner MS, Kennedy TE, Fazeli A, Serafini T, Tessier-Lavigne M, Sretavan DW. Netrin-1 and DCC mediate axon guidance locally at the optic disc: loss of function leads to optic nerve hypoplasia. Neuron. 1997; 19:575–589. [PubMed: 9331350]

Duan X, Qiao M, Bei F, Kim IJ, He Z, Sanes JR. Subtype-Specific Regeneration of Retinal Ganglion Cells following Axotomy: Effects of Osteopontin and mTOR Signaling. Neuron. 2015; 85:1244–1256. [PubMed: 25754821]

Feng G, Mellor RH, Bernstein M, Keller-Peck C, Nguyen QT, Wallace M, Nerbonne JM, Lichtman JW, Sanes JR. Imaging neuronal subsets in transgenic mice expressing multiple spectral variants of GFP. Neuron. 2000; 28:41–51. [PubMed: 11086982]

Fernandes KA, Harder JM, Fornarola LB, Freeman RS, Clark AF, Pang IH, John SW, Libby RT. JNK2 and JNK3 are major regulators of axonal injury-induced retinal ganglion cell death. Neurobiol Dis. 2012; 46:393–401. [PubMed: 22353563]

Fuerst PG, Bruce F, Rounds RP, Erskine L, Burgess RW. Cell autonomy of DSCAM function in retinal development. Dev Biol. 2012; 361:326–337. [PubMed: 22063212]

Fuerst PG, Bruce F, Tian M, Wei W, Elstrott J, Feller MB, Erskine L, Singer JH, Burgess RW. DSCAM and DSCAML1 function in self-avoidance in multiple cell types in the developing mouse retina. Neuron. 2009; 64:484–497. [PubMed: 19945391]

Fuerst PG, Harris BS, Johnson KR, Burgess RW. A novel null allele of mouse DSCAM survives to adulthood on an inbred C3H background with reduced phenotypic variability. Genesis. 2010; 48:578–584. [PubMed: 20715164]

Fuerst PG, Koizumi A, Masland RH, Burgess RW. Neurite arborization and mosaic spacing in the mouse retina require DSCAM. Nature. 2008; 451:470–474. [PubMed: 18216855]

Harder JM, Libby RT. BBC3 (PUMA) regulates developmental apoptosis but not axonal injury induced death in the retina. Mol Neurodegener. 2011; 6:50. [PubMed: 21762490]

Hattori D, Demir E, Kim HW, Viragh E, Zipursky SL, Dickson BJ. Dscam diversity is essential for neuronal wiring and self-recognition. Nature. 2007; 449:223–227. [PubMed: 17851526]

He H, Kise Y, Izadifar A, Urwyler O, Ayaz D, Parthasarthy A, Yan B, Erfurth ML, Dascenco D, Schmucker D. Cell-intrinsic requirement of Dscam1 isoform diversity for axon collateral formation. Science. 2014; 344:1182–1186. [PubMed: 24831526]

Hettinger K, Vikhanskaya F, Poh MK, Lee MK, de Belle I, Zhang JT, Reddy SA, Sabapathy K. c-Jun promotes cellular survival by suppression of PTEN. Cell Death Differ. 2007; 14:218–229. [PubMed: 16676006]

Hughes ME, Bortnick R, Tsubouchi A, Baumer P, Kondo M, Uemura T, Schmucker D. Homophilic Dscam interactions control complex dendrite morphogenesis. Neuron. 2007; 54:417–427. [PubMed: 17481395]

Hummel T, Vasconcelos ML, Clemens JC, Fishilevich Y, Vosshall LB, Zipursky SL. Axonal targeting of olfactory receptor neurons in Drosophila is controlled by Dscam. Neuron. 2003; 37:221–231. [PubMed: 12546818]

Keeley PW, Reese BE. The patterning of retinal horizontal cells: normalizing the regularity index enhances the detection of genomic linkage. Front Neuroanat. 2014; 8:113. [PubMed: 25374512]

Keeley PW, Sliff BJ, Lee SC, Fuerst PG, Burgess RW, Eglen SJ, Reese BE. Neuronal clustering and fasciculation phenotype in Dscam- and Bax-deficient mouse retinas. J Comp Neurol. 2012; 520:1349–1364. [PubMed: 22396220]

Kim JH, Wang X, Coolon R, Ye B. Dscam expression levels determine presynaptic arbor sizes in Drosophila sensory neurons. Neuron. 2013; 78:827–838. [PubMed: 23764288]

Koistinaho J, Hicks KJ, Sagar SM. Long-term induction of c-jun mRNA and Jun protein in rabbit retinal ganglion cells following axotomy or colchicine treatment. J Neurosci Res. 1993; 34:250–255. [PubMed: 8450568]

Koriyama Y, Homma K, Kato S. Activation of cell survival signals in the goldfish retinal ganglion cells after optic nerve injury. Adv Exp Med Biol. 2006; 572:333–337. [PubMed: 17249593]

Li S, Sukeena JM, Simmons AB, Hansen EJ, Nuhn RE, Samuels IS, Fuerst PG. DSCAM Promotes Refinement in the Mouse Retina through Cell Death and Restriction of Exploring Dendrites. J Neurosci. 2015; 35:5640–5654. [PubMed: 25855178]

Libby RT, Li Y, Savinova OV, Barter J, Smith RS, Nickells RW, John SW. Susceptibility to neurodegeneration in a glaucoma is modified by Bax gene dosage. PLoS Genet. 2005; 1:17–26. [PubMed: 16103918]

Liu G, Li W, Wang L, Kar A, Guan KL, Rao Y, Wu JY. DSCAM functions as a netrin receptor in commissural axon pathfinding. Proc Natl Acad Sci U S A. 2009; 106:2951–2956. [PubMed: 19196994]

Ly A, Nikolaev A, Suresh G, Zheng Y, Tessier-Lavigne M, Stein E. DSCAM is a netrin receptor that collaborates with DCC in mediating turning responses to netrin-1. Cell. 2008; 133:1241–1254. [PubMed: 18585357]

McLoon SC, Lund RD. Transient retinofugal pathways in the developing chick. Exp Brain Res. 1982; 45:277–284. [PubMed: 6173249]

Morales Diaz HD. Down syndrome cell adhesion molecule is important for early development in Xenopus tropicalis. Genesis. 2014

Nakazawa T, Shimura M, Tomita H, Akiyama H, Yoshioka Y, Kudou H, Tamai M. Intrinsic activation of PI3K/Akt signaling pathway and its neuroprotective effect against retinal injury. Curr Eye Res. 2003; 26:55–63. [PubMed: 12789537]

Neves G, Chess A. Dscam-mediated self- versus non-self-recognition by individual neurons. Cold Spring Harb Symp Quant Biol. 2004; 69:485–488. [PubMed: 16117684]

Pulverer BJ, Kyriakis JM, Avruch J, Nikolakaki E, Woodgett JR. Phosphorylation of c-jun mediated by MAP kinases. Nature. 1991; 353:670–674. [PubMed: 1922387]

Raivich G, Bohatschek M, Da Costa C, Iwata O, Galiano M, Hristova M, Nateri AS, Makwana M, Riera-Sans L, Wolfer DP, Lipp HP, Aguzzi A, Wagner EF, Behrens A. The AP-1 transcription factor c-Jun is required for efficient axonal regeneration. Neuron. 2004; 43:57–67. [PubMed: 15233917]

Robinson GA, Madison RD. Axotomized mouse retinal ganglion cells containing melanopsin show enhanced survival, but not enhanced axon regrowth into a peripheral nerve graft. Vision Res. 2004; 44:2667–2674. [PubMed: 15358062]

Rockhill RL, Euler T, Masland RH. Spatial order within but not between types of retinal neurons. Proc Natl Acad Sci U S A. 2000; 97:2303–2307. [PubMed: 10688875]

Schmucker D, Clemens JC, Shu H, Worby CA, Xiao J, Muda M, Dixon JE, Zipursky SL. Drosophila Dscam is an axon guidance receptor exhibiting extraordinary molecular diversity. Cell. 2000; 101:671–684. [PubMed: 10892653]

Schramm RD, Li S, Harris BS, Rounds RP, Burgess RW, Ytreberg FM, Fuerst PG. A novel mouse Dscam mutation inhibits localization and shedding of DSCAM. PLoS One. 2012; 7:e52652. [PubMed: 23300735]

Stacy RC, Wong RO. Developmental relationship between cholinergic amacrine cell processes and ganglion cell dendrites of the mouse retina. J Comp Neurol. 2003; 456:154–166. [PubMed: 12509872]

Sun F, Park KK, Belin S, Wang D, Lu T, Chen G, Zhang K, Yeung C, Feng G, Yankner BA, He Z. Sustained axon regeneration induced by co-deletion of PTEN and SOCS3. Nature. 2011; 480:372–375. [PubMed: 22056987]

Vander S, Levkovitch-Verbin H. Regulation of cell death and survival pathways in secondary degeneration of the optic nerve - a long-term study. Curr Eye Res. 2012; 37:740–748. [PubMed: 22631427]

Wang J, Zugates CT, Liang IH, Lee CH, Lee T. Drosophila Dscam is required for divergent segregation of sister branches and suppresses ectopic bifurcation of axons. Neuron. 2002; 33:559–571. [PubMed: 11856530]

Wassle H, Riemann HJ. The mosaic of nerve cells in the mammalian retina. Proc R Soc Lond B Biol Sci. 1978; 200:441–461. [PubMed: 26058]

Watkins TA, Wang B, Huntwork-Rodriguez S, Yang J, Jiang Z, Eastham-Anderson J, Modrusan Z, Kaminker JS, Tessier-Lavigne M, Lewcock JW. DLK initiates a transcriptional program that couples apoptotic and regenerative responses to axonal injury. Proc Natl Acad Sci U S A. 2013; 110:4039–4044. [PubMed: 23431164]

Xu Y, Ye H, Shen Y, Xu Q, Zhu L, Liu J, Wu JY. Dscam mutation leads to hydrocephalus and decreased motor function. Protein Cell. 2011; 2:647–655. [PubMed: 21904980]

Yamagata M, Sanes JR. Dscam and Sidekick proteins direct lamina-specific synaptic connections in vertebrate retina. Nature. 2008; 451:465–469. [PubMed: 18216854]

Yamakawa K, Huot YK, Haendelt MA, Hubert R, Chen XN, Lyons GE, Korenberg JR. DSCAM: a novel member of the immunoglobulin superfamily maps in a Down syndrome region and is involved in the development of the nervous system. Hum Mol Genet. 1998; 7:227–237. [PubMed: 9426258]

Yang J, Wu Z, Renier N, Simon DJ, Uryu K, Park DS, Greer PA, Tournier C, Davis RJ, Tessier-Lavigne M. Pathological axonal death through a MAPK cascade that triggers a local energy deficit. Cell. 2015; 160:161–176. [PubMed: 25594179]

Yimlamai D, Konnikova L, Moss LG, Jay DG. The zebrafish down syndrome cell adhesion molecule is involved in cell movement during embryogenesis. Dev Biol. 2005; 279:44–57. [PubMed: 15708557]

Yoshida K, Behrens A, Le-Niculescu H, Wagner EF, Harada T, Imaki J, Ohno S, Karin M. Amino-terminal phosphorylation of c-Jun regulates apoptosis in the retinal ganglion cells by optic nerve transection. Invest Ophthalmol Vis Sci. 2002; 43:1631–1635. [PubMed: 11980884]

Highlights

- Retinal ganglion cell axon stress is observed after eye opening in Dscam mutant mice
- Axons subsequently make extensive projections within the mutant retina
- This phenotype is observed in the Bax mutant retina and is not the result of damage to central targets
- Activation of stress markers associated with glaucoma and optic nerve crush such as JUN and JNK are observed in the *Dscam* mutant retina
- Deletion of *Jun* increases axon remodeling

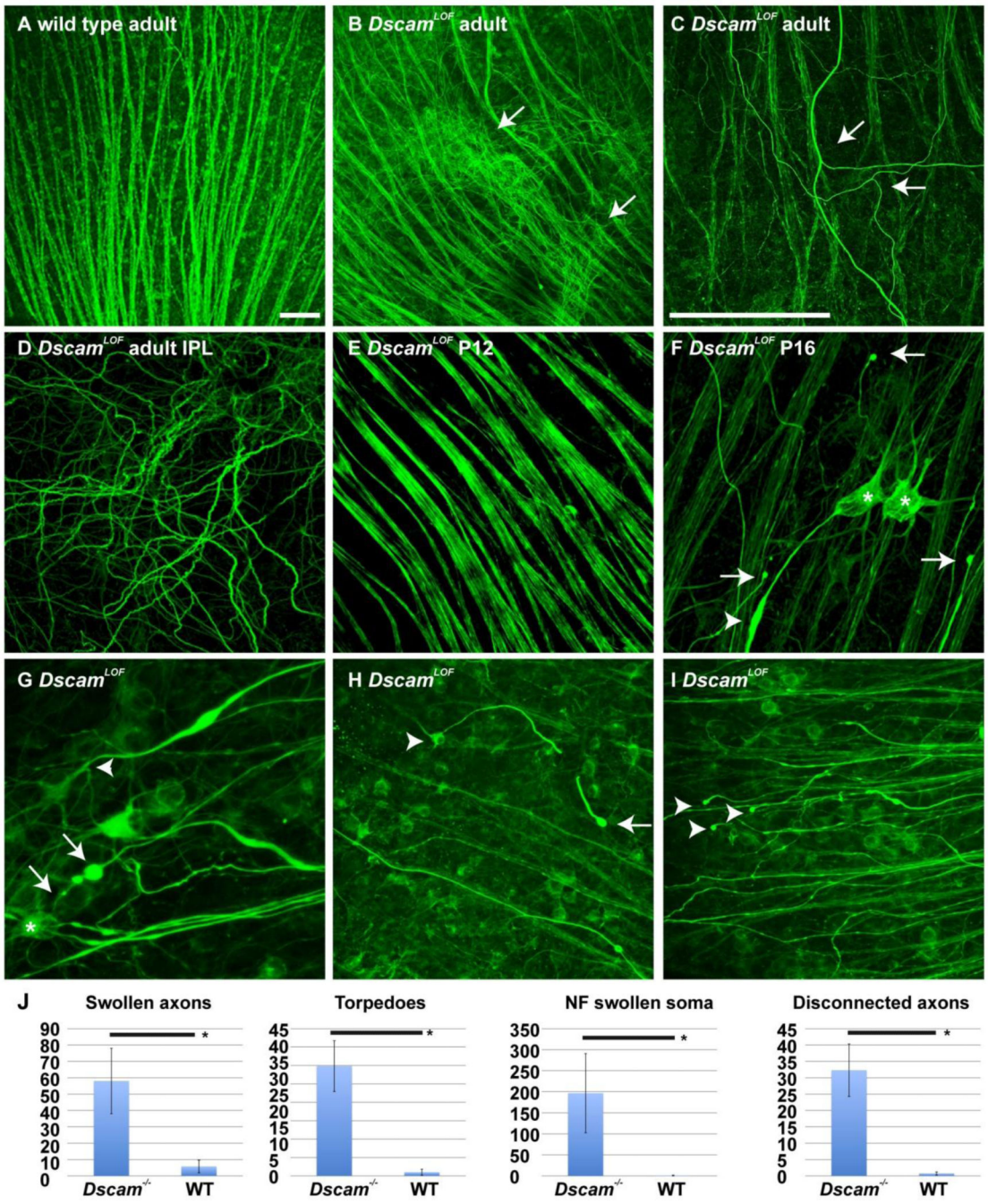

Figure 1. Postnatal axon branching and stress in *Dscam*^{LOF} mice

Wild type and *Dscam*^{LOF} retinas stained with antibodies to neurofilament medium chain protein. **A** and **B**, Abnormal projection of retinal ganglion cell (RGC) axons was observed in the *Dscam*^{LOF} retina (**B**: arrows). **C**, Abnormal axon branching was observed in the peripheral retina (arrows). **D**, Abnormal axons were observed to project through the inner plexiform layer (IPL) of the *Dscam*^{LOF} retina. **E**, Axon morphology in *Dscam*^{LOF} mice was normal prior to eye opening, which occurs after postnatal day 12 (P12). **F**, Signs of axon stress, including accumulation of neurofilament protein in the cell soma (asterisks), blebbing

of axons (arrows), and swollen axon torpedoes (arrow head), were observed in *Dscam*^{LOF} mice by P16. **G**, Swollen axons with torpedoes (arrows) and branching (arrowhead). **H**, RGC (arrowhead) with a broken axon that terminates in a bleb (arrow). **I**, Axons not visibly connected to RGC soma that terminate in blebs. N>3 at all ages. **J**, The number of swollen axons, axon torpedoes, neurofilament (NF) swollen somata and disconnected axons were significantly increased in *Dscam*^{LOF} retinas compared to wild type controls at P16 (Student's *t*-test < 0.01). **A**-**F** *Dscam*^{del17}, **G**-**I** *Dscam*^{2J} and sibling controls used. N≥6. Scale bar (in **A**) = 50 μm; **A**, **B**, (in **C**) = 25 μm **C**-**F**, (in **C**) = 50 μm; **G**, (in **C**) = 100 μm; **H** and **I**.

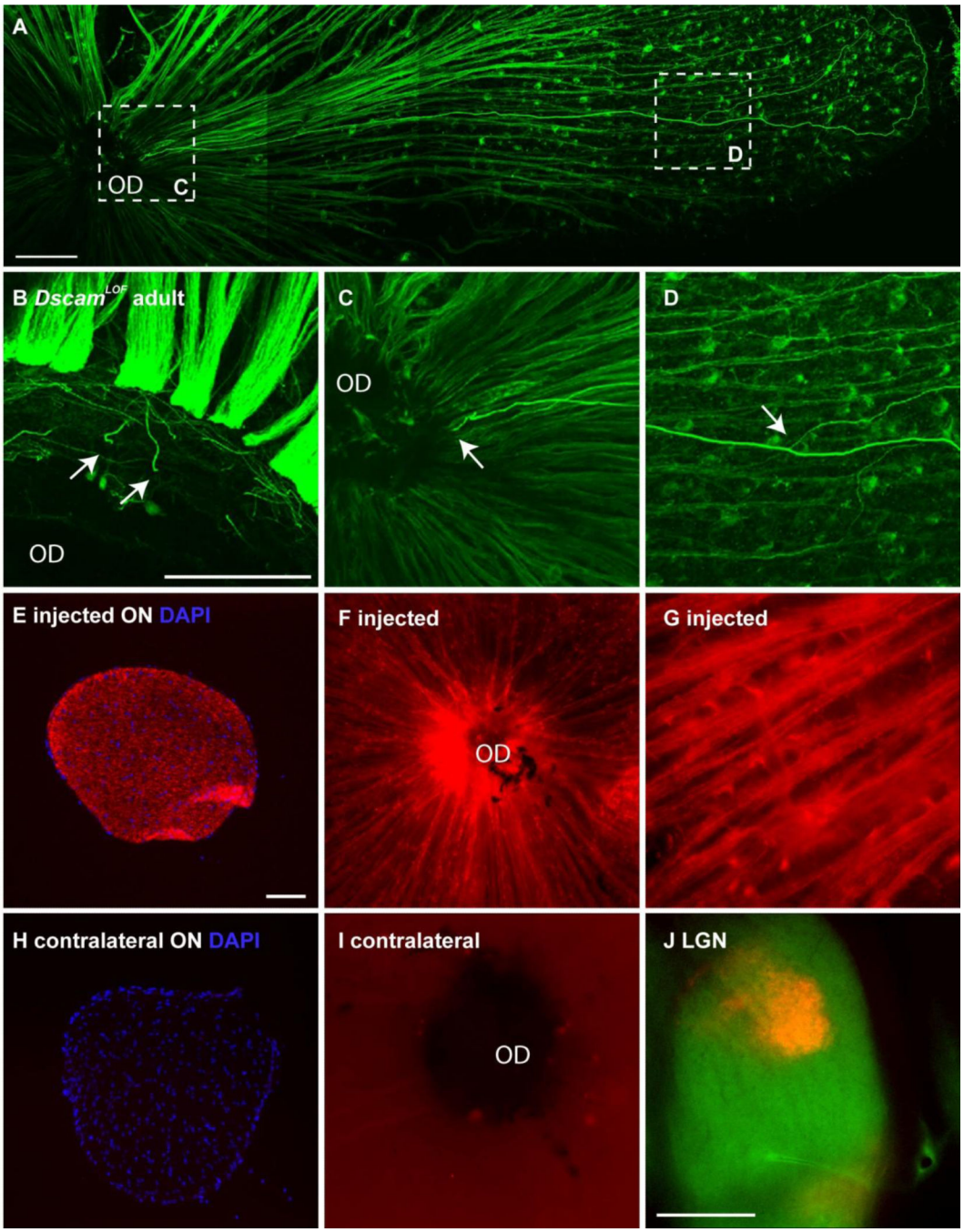

Figure 2. Origin of misprojecting axons

A-**D**, *Dscam*^{LOF} retina stained with antibodies to neurofilament. **A**, Abnormal axons appear to project out of the optic disc (OD). **B**, Cut section at the level of the optic disc shows multiple axons (arrows). **C**, Higher magnification image of left inset from **A** showing swollen axon (arrow). **D**, Higher magnification of inset in **A** showing axon branching in peripheral retina (arrow). **E**-**G**, Optic nerve (ON) (**E**) and retina (**F** and **G**) of eye injected with alexa-conjugated cholera toxin. **H** and **I**, Optic nerve and retina of contralateral eye showing no fluorescence. **J**, Cholera toxin trafficked to distal axonal targets normally.

N>10: **A**-**D**, N=6: **E**-**J**. *Dscam*^{FD} mice used. Scale bar (in **A**) = 100 μm; **A**, (in **B**) = 100 μm; **B**, **C**, **D**, **G**, (in **E**) = 100 μm; **E**, **F**, **H**, **I**, (in **J**) = 400 μm.

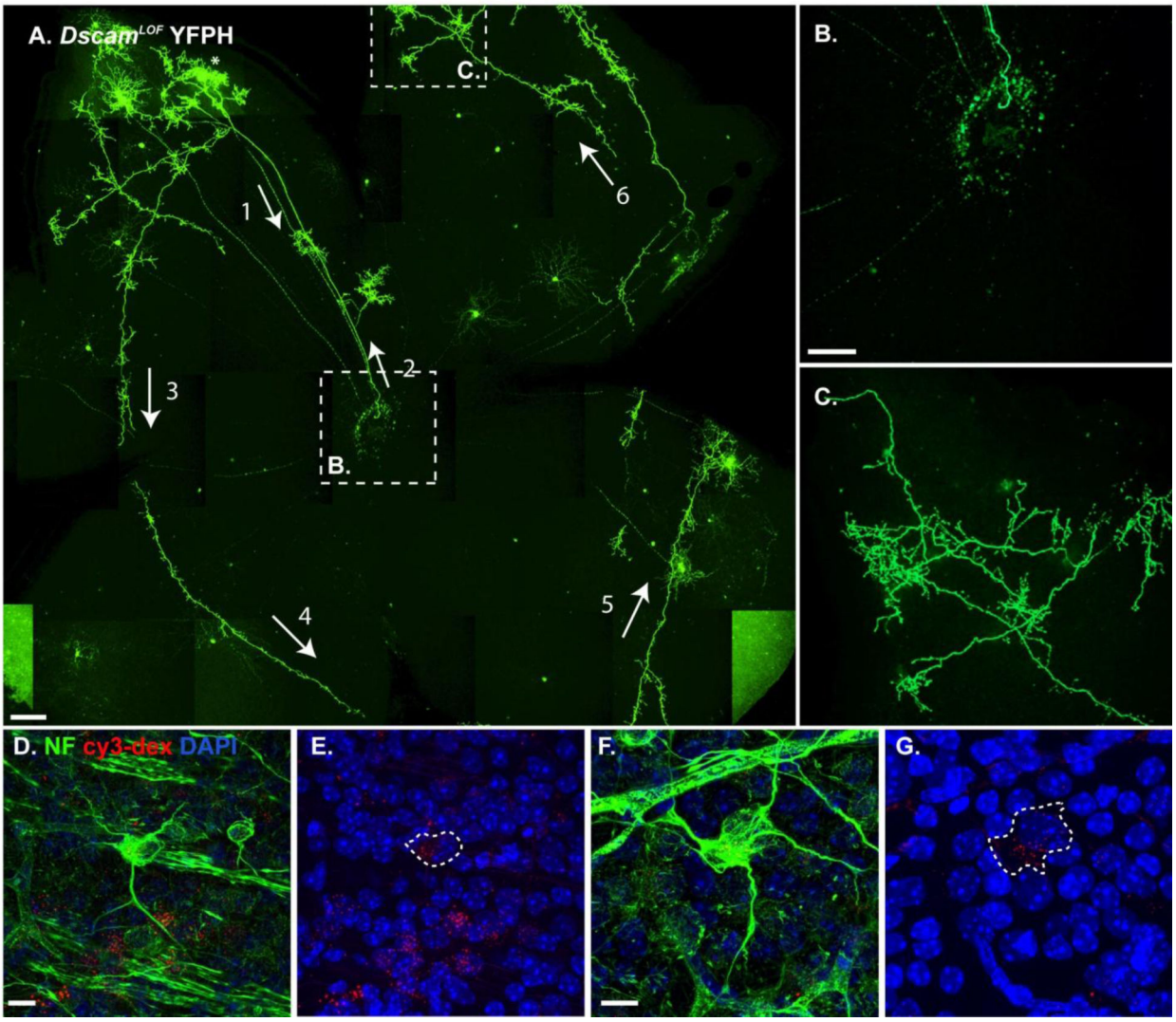

Figure 3. Single cell analysis indicates that abnormal axons project across the *Dscam*^{LOF} retina

A-C, Confocal z-projection of a *Dscam*^{LOF} retina carrying the YFPH transgene revealed the extensive projections that a single RGC axon could make. **A**, An abnormal axon projects from an RGC towards the optic disc (1: arrow), where it turns around and projects back into the retina (2: arrow and **B**). The axon then projects around the retina (3-6: arrows) and makes collateral branches that send terminals into the plexus layers of the retina (**C**). **D-G**, Retinas of *Dscam*^{LOF} mice stained with antibodies to neurofilament after fluorescent dextran was injected into the superior colliculus. Fluorescent dextran was observed in the soma of cells that had accumulated neurofilament. Dashed rings show the outline of neurofilament filled soma (**E** and **G**). N>20 retinas A-C. N>3: D-G. Abbreviations: NF: neurofilament, cy3-dex: fluorescently labeled dextran. **A-G**: *Dscam*^{del17} strain used. Scale bar (in **A**) = 200 μm, (in **B**) = 100 μm: **B**, **C**, (in **D**) = 10 μm: **D**, **E**, (in **F**) = 10 μm: **F**, **G**.

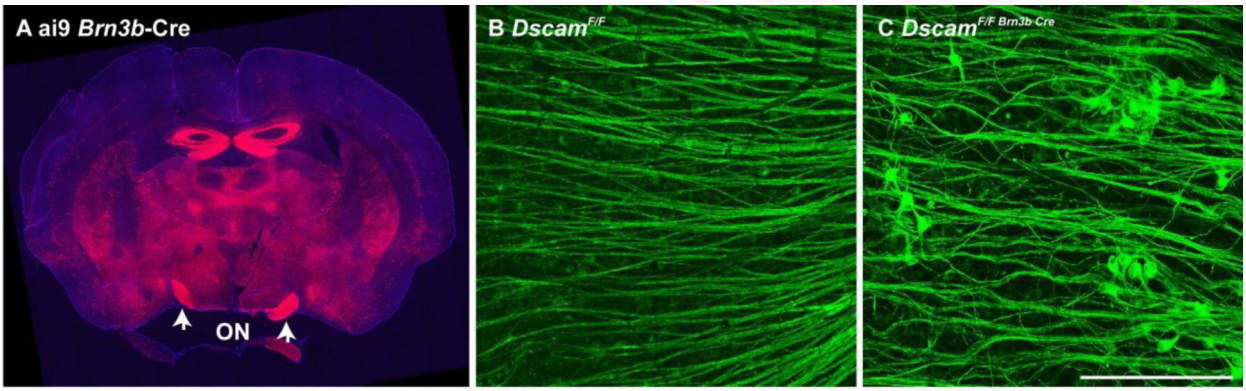

Figure 4. Hydrocephalus in *Dscam* mutant mice is not necessary to cause axon remodeling

A, *Dscam* was conditionally targeted with *Brn3b*-Cre, which is expressed in the midbrain and retina, but does not result in hydrocephalus, as visualized with the ai9 reporter. **B** and **C**, Axon remodeling was observed after conditionally targeting *Dscam* with *Brn3b*-Cre (C) but not in Cre-negative controls (B). N≥3. Scale bar (in **B**) **B**-**H** = 100 μm in B and C.

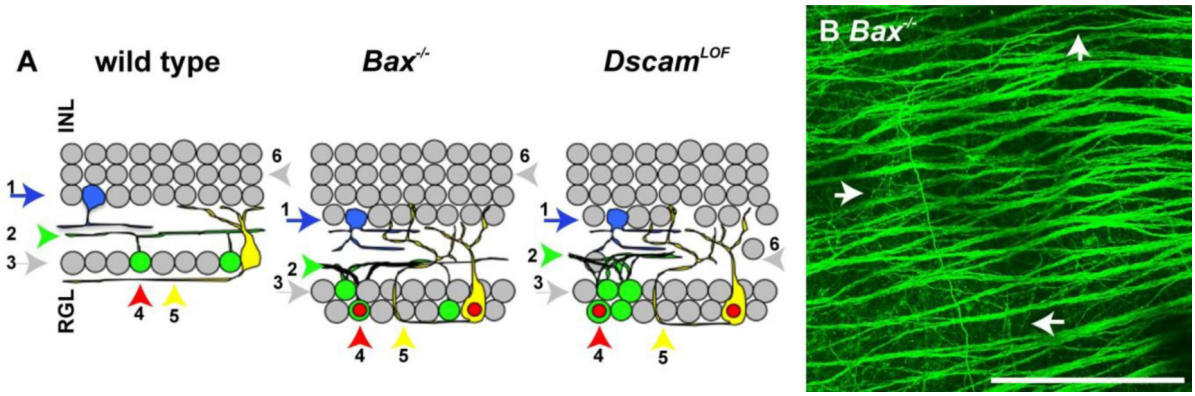

Figure 5. *Bax* null retina phenocopies RGC and axon misprojection phenotype observed in the *Dscam* null retina

Cartoon summarizing differences and similarities between the wild type, *Bax* null and *Dscam* mutant retina. **A**, Defects in dendrite lamination (1), RGC dendrite clumping (2), a decrease in developmental cell death (3), activation of JUN (4), and misprojection of axons (5) are observed in both the *Dscam* and *Bax* null retina compared to wild type. Uneven soma lamination (6) is observed in the *Dscam* mutant retina, but not in the *Bax* null or wild type retina. **B**, Misprojected axons were observed in the *Bax* null retina. N=4: A-E. Scale bar (in B) = 50 μm.

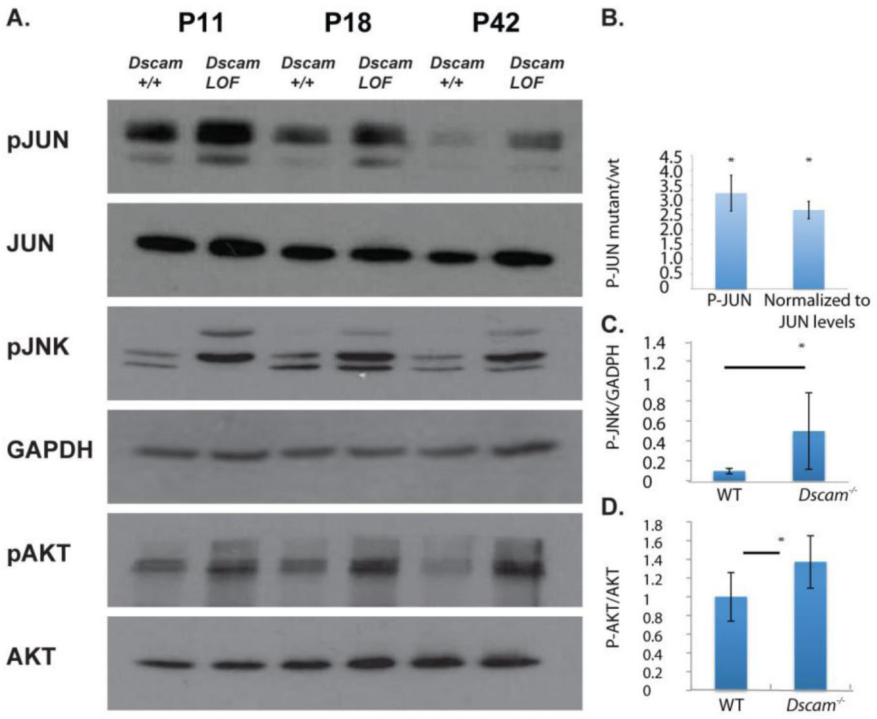

Figure 6. Increased activation of cell stress associated proteins in *Dscam*^{LOF} mice

A, Western blot analysis of retinal lysates from *Dscam* mutant mice and controls at postnatal day 11 (P11), P18 and P42. Blots were probed with antibodies to phosphorylated JUN (pJUN), JUN, phosphorylated JNK (pJNK), phosphorylated AKT (pAKT), AKT and GAPDH, as an additional loading control. An increase in the activation state of JUN, JNK and AKT was observed in *Dscam* mutant mice. **B**, PJUN levels were significantly increased in *Dscam*^{LOF} retinas compared to wild type. **C**, PJNK levels were significantly increased in *Dscam*^{LOF} retinas compared to wild type. **D**, pAKT levels, normalized to total AKT levels, were significantly increased in *Dscam*^{LOF} retinas compared to wild type. N=4 in B, =3 in other panels. B assayed at postnatal day 14. C and D assayed at postnatal day 18. *Dscam*^{2J} mice and wild type sibling controls used.

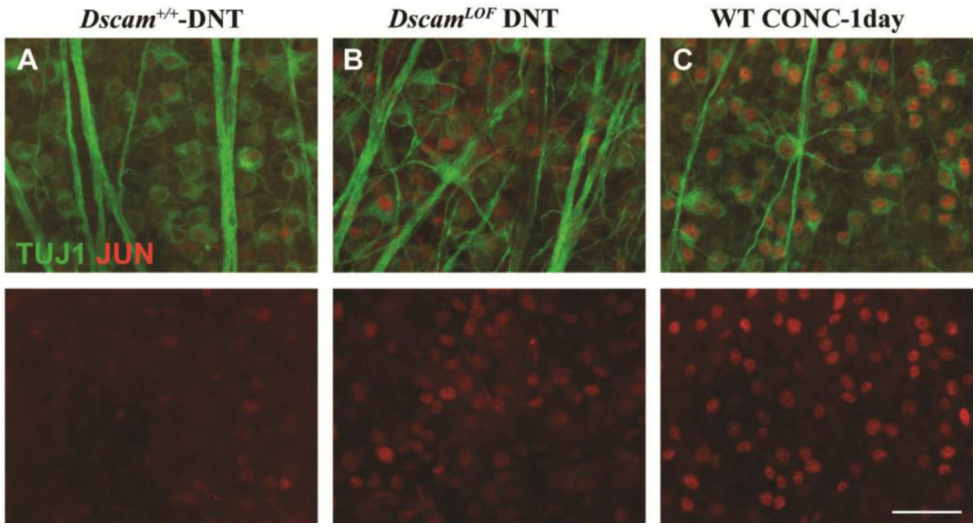

Figure 7. JUN upregulation in *Dscam*^{LOF} mice

Retinas were stained with antibodies to JUN and TUJ1. **A**, A few JUN positive cells are observed in wild type retinas. **B**, A large number of RGCs are JUN-positive in the *Dscam*^{LOF} retinas. **C**, Wild type retina showing the upregulation of JUN in all RGCs after an acute axonal insult, optic nerve crush. N>3. The scale bar is equivalent to 50 μm.

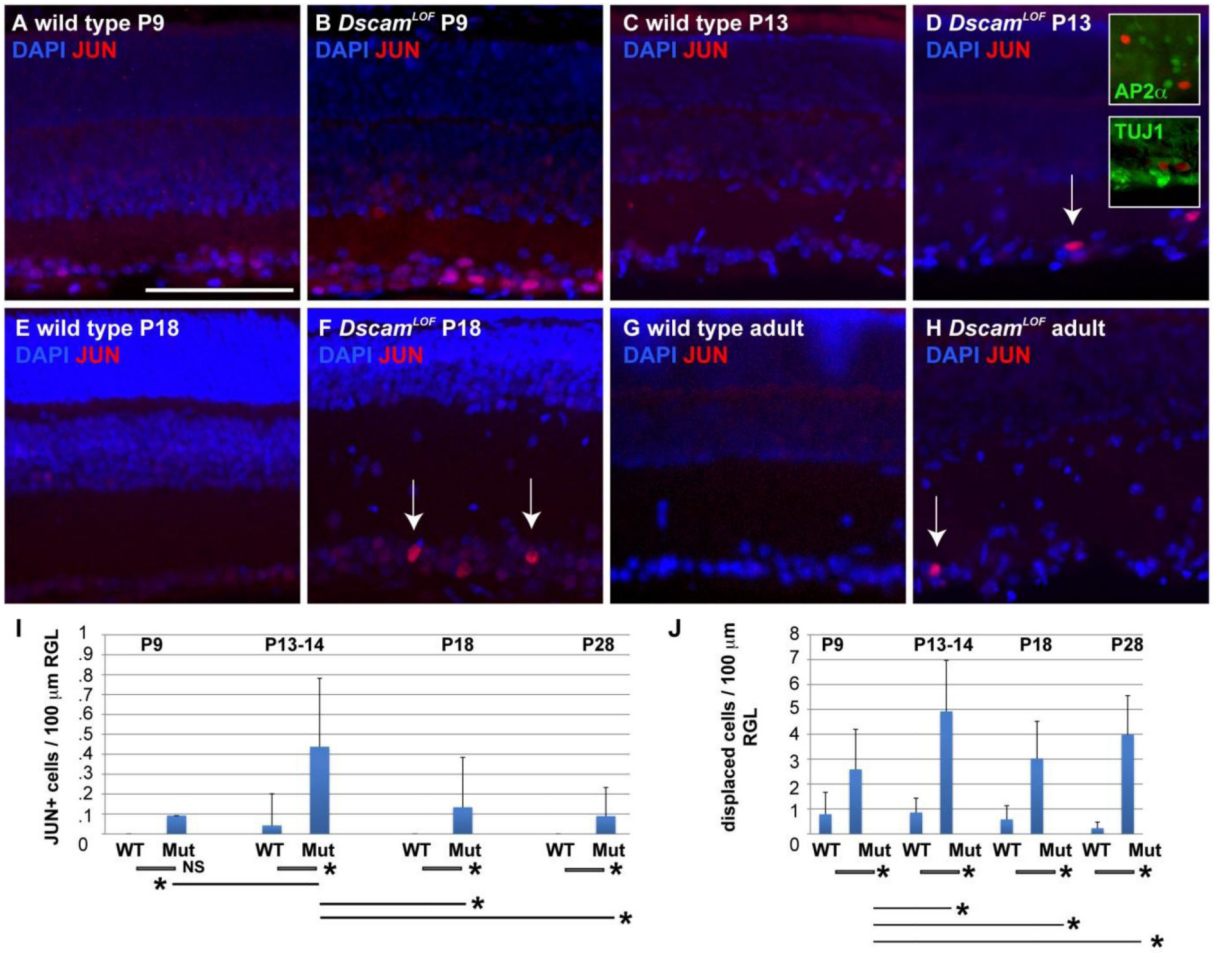

Figure 8. JUN levels are increased in a small number of *Dscam*^{LOF} RGCs

An antibody to JUN was used to assay localization at postnatal (P) day 9, 13/14, 18 and in the adult retina. Accumulation of JUN was observed in RGCs in the *Dscam*^{LOF} retina at and after P9 (arrows). Double staining with a pan-amacrine cell marker (AP2α) and a pan-ganglion cell marker (TUJ1) confirmed that these were RGCs. N=3 retinas at each age. **I**, Quantification of cJUN+ cells. A significant increase in the number of cJUN+ cells was observed comparing the wild type and *Dscam*^{LOF} retina at P13/14 (retinas were pooled from P13 and P14 ages to gain a sufficient N), P18, and in the adult retina (Student's *t*-test value, not significant (NS) at P9, <0.001; P13/14 and P18; 0.03 comparing adult retina). No significant change was detected comparing wild type retinas at different ages. A significant increase in the number of cJUN+ cells was detected in the *Dscam*^{LOF} retina at P13/14 compared to other tested *Dscam*^{LOF} ages (Student's *t*-test p value < 0.001), but not when comparing other ages to each other (i.e., P18 *Dscam*^{LOF} vs. adult *Dscam*^{LOF}). **J**, A significant increase in the number of displaced cells was detected comparing wild type and *Dscam*^{LOF} retinas at all ages (Student's *t*-test < 0.0001). A significant increase in the number of displaced cells was also detected when comparing older *Dscam*^{LOF} retinas to P9 *Dscam*^{LOF} retinas (Student's *t*-test < 0.002). N≥3. Scale bar in (**A**) = 100 µm. Insets=37.5 µm.

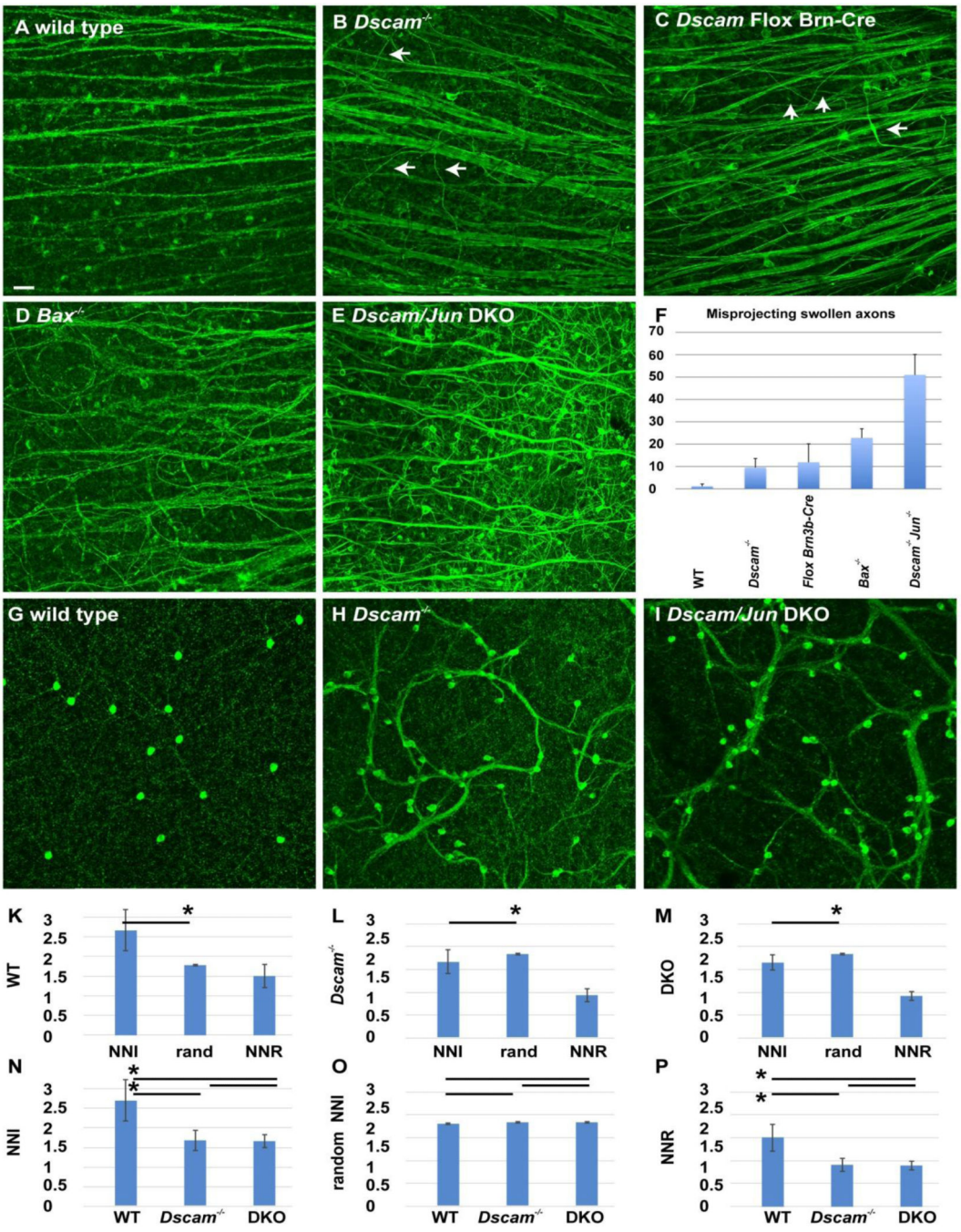

Figure 9. Deletion of JUN increases number of misprojected axons in the *Dscam*^{LOF} retina

A-E, Wild type and mutant genotypes. *Dscam* and *Jun* were conditionally deleted using *Six3*-Cre. **F,** Quantification of axon misprojection. A significant increase in misprojected axons was detected in all genotypes compared to wild type. An increase in the number of misprojecting axons was detected in the *Bax* mutant retina compared to *Dscam*^{LOF} retinas. A significant increase in the number of misprojecting axons was detected in the *Dscam*/*Jun* double mutant retina compared to all other genotypes. **G-I**, *Dscam* loss-of-function dendrite clustering phenotype of TH-positive dopaminergic amacrine (DA) cells in the IPL was still

observed in the absence of *Jun*. N=4 (4 retinas). **K**-**P**, Nearest neighbor analysis of DA cells was performed in wild type, *Dscam*^{LOF} and *Dscam*/*Jun* (DKO) mutant retinas. Nearest neighbor index (NNI) values reflect the degree of spacing compared to the most optimal space-filling model, that is a hexagonal organization. Nearest neighbor ratio (NNR) values control for cell density by dividing the actual NNI by the random NNI, generated by randomly distributing a like number of cells averaged over 500 trials. **K**, Wild type NNI values were significantly increased compared to random simulations (Student's *t*-test p-value <0.001), indicating a greater degree of spatial organization compared to a random distribution. **L**, *Dscam*^{LOF} DA cell NNI values were significantly decreased compared to random (Student's *t*-test p-value <0.03). **M**, DA cells in the *Dscam*/*Jun* DKO mutant mice had a significantly lower NNI values compared to controls (Student's *t*-test p-value <0.01). **N**, Comparison of NNI values across genotypes. NNI values were significantly increased in wild type compared to single or double mutants (Student's *t*-test p-value <0.001), while no significant difference was observed comparing *Dscam* and *Dscam*/*Jun* NNI values. **O**, No significant differences in NNI values were detected when comparing the random simulation of density-matched spacing for each genotype. **P**, Nearest neighbor ratio (NNR) values, which normalize for cell density, were significantly different comparing wild type to either mutant genotypes (Student's *t*-test p-value <0.001), but the *Dscam*^{LOF} and DKO NNR values were not significantly different from each other. N≥4. P-values for axon misprojection phenotype are listed in Table 1. Scale bar (in **A**) **A**-**G** = 50 μm.

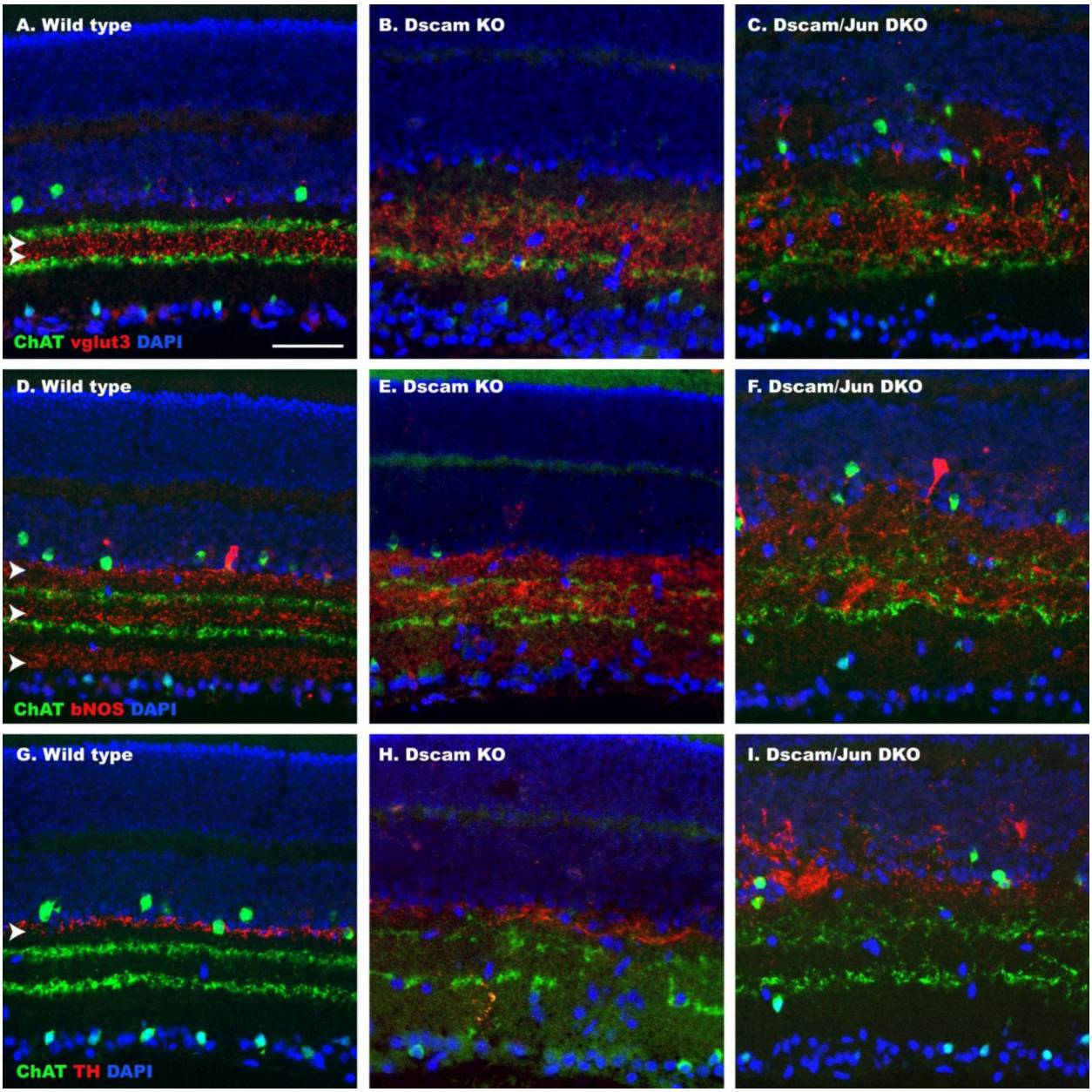

Figure 10. Neurite Lamination in the *Dscam*/*Jun* double mutant retina

Sections of wild type, *Dscam*^{LOF} and *Dscam*/*Jun* (DKO) mutant retinas stained with amacrine cell markers to visual neurite stratification. **A-C**, Sections labeled with antibodies to ChAT and vglut3. Vglut3 staining is normally concentrated between ChAT staining (A; arrowheads). Vglut3 lamination is disrupted in the *Dscam*^{LOF} and *Dscam*/*Jun* mutant retinas compared to wild type. **D-F**, Sections labeled with antibodies to ChAT and bNOS. BNOS staining is normally localized in three discreet bands (D; arrow heads). Lamination is disrupted in the *Dscam*^{LOF} and *Dscam*/*Jun* mutant retinas compared to wild type. **G-I**, Sections labeled with antibodies to ChAT and TH. TH staining normally is limited to the border between the inner nuclear layer and inner plexiform layer (G; arrowhead).

Lamination is disrupted in the *Dscam*^{LOF} and *Dscam*/*Jun* mutant retinas compared to wild type. Scale bar (in A) = 50 μm.

Table 1

Adult mistargeted axons

Genotype	Axons*	n retinas	v. wt p	v. KO p	v. Brn p	v. Bax p	v. DKO p
Wild type	1.1±1.1	28		≥0.001	≥0.001	=0.001	≥0.001
Dscam mutant	9.6± 4.0	16			= .36	≥0.001	≥0.001
Dscam floxed Brn Cre	11.8±8.3	8				≥0.019	≥0.001
Bax mutant	22.8±4.1	5					≥0.001
Dscam/*Jun* mutant	51±9.1	5					

* The number of swollen axons misprojecting through the retina beginning at the optic disc